A comparison of kinematic evidence for tropical cells in the Atlantic and Pacific oceans

R. L. Molinari [a]*, S. Bauer [b], D. Snowden [a], G. C. Johnson [c], B. Bourles [d], Y. Gouriou [e], H. Mercier [f]

[a] National Oceanic and Atmospheric Administration Atlantic Oceanographic and Meteorological Laboratory, 4301 Rickenbacker Causeway, Miami, Florida 33149, USA

[b] University of Miami, Cooperative Institute for Marine and Atmospheric Studies, Miami, Florida 33149, USA

[c] National Oceanic and Atmospheric Administration Pacific Marine Environmental Laboratory, Seattle, WA, USA

[d] Institut de Recherche pour le Developpement Brest, France

[e] Institut de Recherche pour le Developpement Noumea, New Caledonia

[f] Centre National de la Recherche Scientifique, Institut Francais de Recherches pour L'Exploitaton de la Mer Plouzane, France

Kinematic evidence for the existence of Tropical Cells (TC) in the Atlantic Ocean is offered. Mean sections of meridional velocity, its horizontal divergence and vertical velocity are estimated from twelve available sections centered at about 35ºW. Of the twelve sections, six were occupied in March and April, thus there is a boreal spring bias to the observations. Equatorial upwelling and off-equatorial downwelling, between 3ºN and 6ºN, represent the southern and northern boundaries of a northern hemisphere TC. Uncertainties for the estimates of average quantities are large. However, favorable comparisons with observational representations of Pacific TC's provide support for the existence of a northern hemisphere Atlantic TC.

1. INTRODUCTION

In the Pacific and Atlantic Oceans, meridional-vertical circulation is a superposition of larger Subtropical Cells (STCs) and more localized Tropical

* Corresponding author. Tel: +1-305-361-4873. Fax: +1-305-361-4701. Email address: Bob.Molinari@noaa.gov

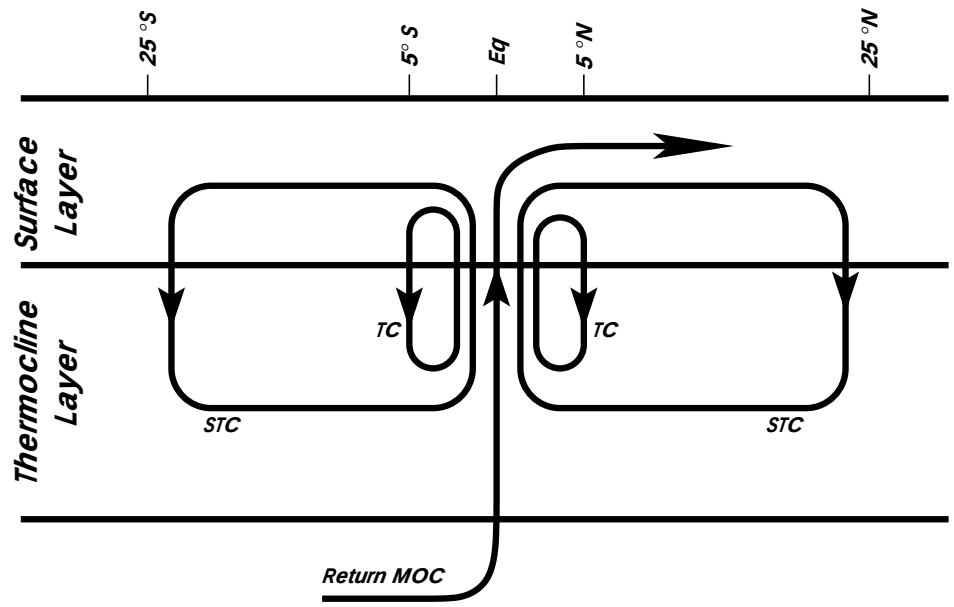

Figure 1. Schematic diagram representing the structure of Tropical Cells and Subtropical Cells as modeled by and modified from Lu *et al*. (1998).

Cells (TCs' Johnson *et al*., 1998; Johnson *et al*., 2001; Johns, 2001). These cells share equatorial upwelling, caused by Ekman divergences and poleward surface Ekman flow (Figure1). The TC downwelling is located in surface convergence zones observed about 4 - 8 degrees from the equator. Completing the TC, this water is probably returned to the equator in the interior of the basin and at depths no deeper than the upper thermocline. The STCs extend to the subtropics where subduction causes a downwelling that reaches to greater densities than that of the TCs. STC transport to the equator occurs both along the western boundary and in the interior. Although the name TC is a recent addition to oceanographic terminology, in fact, these features have a long history. As described in Sverdrup *et al.* (1942), Defant (1936) characterized a TC in the North Atlantic located between the Equatorial Undercurrent (EUC) and the North Equatorial Countercurrent (NECC). Defant (1936) proposed that frictional forces acting between the equatorial currents caused the TC.

In the Pacific, Wyrtki and Kilonsky (1984) analyzed data from about 30 cross-equatorial hydrographic sections from ten cruises taken over 12 months during the Hawaii-to Tahiti Shuttle Program. They inferred upwelling at the equator and downwelling at 4ºN from water-mass property distributions. They went on to argue that the downwelling is caused by convergence in the wind-driven surface Ekman transport. Johnson and Luther (1994) using a subset of the Hawaii-to-Tahiti Shuttle Acoustic Doppler Current Profiler (ADCP) data, estimated a similar, but statistically uncertain, pattern of near-equatorial upwelling and off-equatorial downwelling. Johnson *et al.* (2001), hereinafter JMF, used shipboard ADCP (SADCP) data to study equatorial Pacific circulation. They considered 85

cross-equatorial sections occupied over a ten-year period between 170ºW and 95ºW. They derived average vertical sections of the horizontal velocity components, horizontal divergence, and vertical velocity at a nominal longitude of 136ºW, the approximate mid-longitude of their data. They find upwelling in the equatorial band as well as downwelling between 4ºS and 6ºS and 6ºN and 9ºN. Surface drifter data have also been used to diagnose near-surface divergence fields. They show upwelling near the equator and downwelling near 4ºS and 4ºN (Johnson, 2003). The downwelling regions represent the poleward boundaries of the Pacific TC's in both data sets.

Herein, we search for kinematic evidence for TC's in the tropical Atlantic Ocean using similar data and analyses to that employed by JMF in the Pacific. We begin with a description of the data and analyses used, followed by estimates of the mean zonal velocity structure. Average meridional velocity, it's horizontal divergence, and vertical velocity transects are then given. The vertical velocities are used to estimate upwelling transports. Throughout the discussion, we compare Atlantic characteristics with those of JMF both to support the Atlantic results and to consider the ubiquity of the TC feature. We conclude with a discussion of sampling and unresolved issues.

2. DATA AND ANALYSES

Twelve SADCP sections occupied in the western equatorial Atlantic between 40ºW and 30ºW are used in this study (Figure 2). The characteristics of these sections are summarized in Table 1. Spatially, they vary in (1) latitudinal extent within the band 7ºS to 7ºN; (2) shallowest depth resolved, 20m to 40m; and (3) deepest depth available, 200m to 400m. Figure 3 shows the availability of data by depth and latitude. Maximum coverage is between 30m and 200m and 4ºS and 6ºN, which are limits used for most of our analyses. Temporally, more than half of the cruises are in early boreal spring, with the rest spread over the remainder of the year (Table 1).

The SADCP data were acquired from the World Ocean Circulation Experiment (WOCE) SADCP Data Assembly Center in Honolulu, Hawaii, except for the THALASSA, 1999 and OCEANUS 2000 cruises, provided by the principal investigators. Analyses procedures for each cruise varied (e.g., Wilson *et al.*, 1994 and Bourles *et al.*, 1999). However, qualitatively, SADCP uncertainties are largest in the cross-stream direction (zonal in the case of these sections) and are of the order 0.05-0.10 m/s (JMF).

The average zonal current structure of the western tropical Atlantic is computed from the SADCP data and compared with similar structure in the Pacific. The comparison serves two purposes: (1) it provides qualitative support for the results derived from the limited number of Atlantic sections (12 versus 85 in the Pacific, JMF); and (2) provides validation information for global modelers who simulate the tropics. Volume transports were estimated for the EUC and

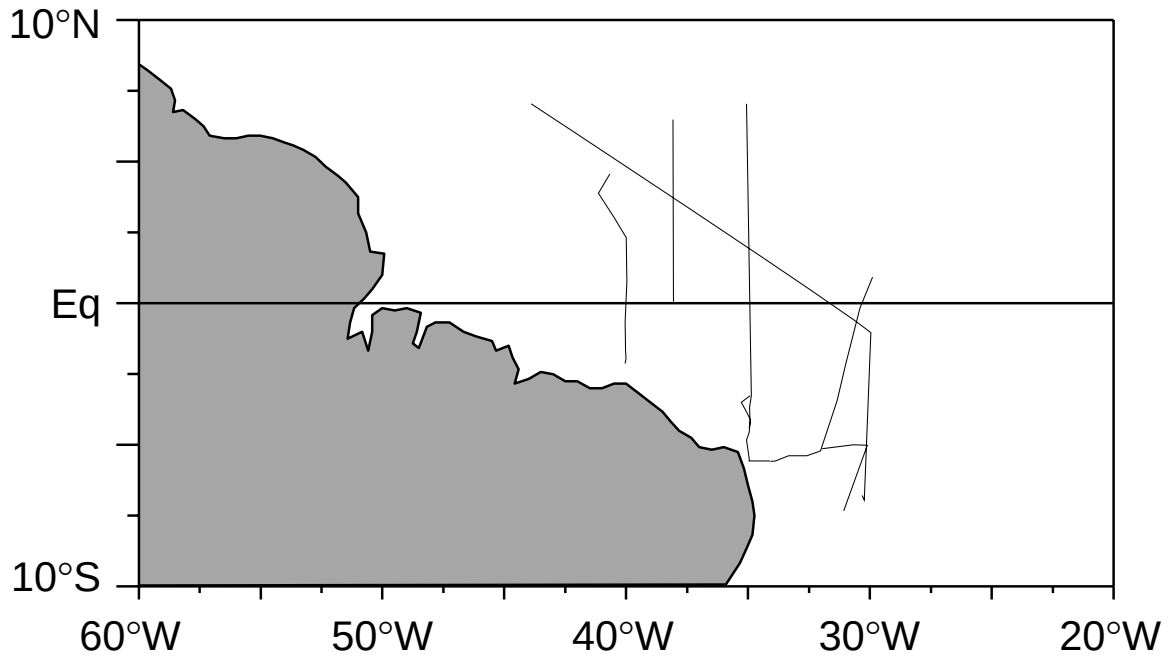

Figure 2. Locations of the sections used in this study.

Table 1.
Description of hull mounted ADCP sections

VESSEL	DATE DEEPEST	LONGITUDE	LATITUDE RANGE	SHALLOWEST DEPTH	DEPTH
L'ATALANTE	Jan. 31 - Feb.5 "93	35ºW	5.58°S - 7.00°N	28m	700m
METEOR	May 29 - Jun.3 "91	35ºW	5.61°S - 2.45°N	28m	330m
METEOR	Nov. 1 - 5 "92	35ºW	4.97°S - 3.97°N	29m	400m
METEOR	Mar.12 - 16 "92	35ºW	4.81°S - 4.50°N	32m	400m
EDWIN A. LINK	Apr.26 - May 1"96	35ºW	4.78°S - 7.00°N	16m	340m
METEOR	Jun.7 - 9 "91	30ºW	5.25°S - 0.87°N	28m	330m
MAURICE EWING	Mar. 1 - 8 "94	30ºW	6.98°S - 0.99°S	26m	390m
		30ºW	0.99°S		
		43.8ºW	7.00°N		
METEOR	Mar. 6 - 10 "94	40ºW	2.00°S - 4.47°N	26m	400m
OCEANUS	Mar. 7 - 15 "01	35ºW	0.60°S - 6.80°N	23m	400m
		38ºW	.0°S - 6.40°N	23m	400m
THALASSA	Jul. 19 - 29 "99	35ºW	5.59°S - 6.99°N	30m	700m

North and South Equatorial Undercurrents (NEUC and SEUC), these are often called the North and South Subsurface Countercurrents in the Pacific. For each cruise, the transports for each current were computed within the areas bounded by either 300m, the surface in the case of the EUC and/or the 0 m/s speed contour.

Meridional velocity, it's horizontal divergence and vertical velocity sections were estimated for each cruise (using a one-degree of latitude by 10 m grid). To obtain near-surface values of meridional velocity in their Pacific work, JMF used objective mapping to extrapolate vertical shear from the top few SADCP bins to the surface. For the Atlantic, we use the more conservative estimate of no vertical shear above 30m (or 40m when required) and thus simply extrapolate this meridional velocity to the surface. Differences between the two approaches of extrapolation can lead to different estimates of volume transport as shown by Marin and Gouriou (2000). They computed a 1.4 Sv (1 Sv = 10^6 m^3/s), 20%, difference in directly observed Ekman volume transport through the upper 100m of a trans-Atlantic section at 7.5ºN. However, because of the many complicating factors that contribute to the vertical structure of near-surface velocity in the tropics (e.g., thermocline depth, mixed layer depth, etc.), it is difficult to select quantitatively the best approach for extrapolation to the surface. In the Pacific, JMF have the necessary spatial fields of zonal and meridional velocity components to compute both terms in the expression for horizontal divergence. In the Atlantic, there are insufficient SADCP data zonally to compute representative estimates of $\partial u/\partial x$. Thus the divergence sections are estimated from only the meridional velocity. The adequacy of this assumption is discussed in the next section. To estimate vertical velocity sections, we then integrate the divergences with respect to depth assuming a rigid lid at the sea surface.

The individual sections were averaged to estimate mean transects for each variable. In addition, a section of the standard error of the mean for the meridional velocity was computed from the individual transects to provide a measure of the uncertainty in the results. Implicit in this uncertainty method is the assumption that instrument errors are much less than geophysical noise as in JMF. This minimum measure of uncertainty was used because of the few sections available for analysis.

The small signal-to-noise ratio in the meridional velocity field, to be described, results in extended areas of larger uncertainty in the divergence and vertical velocity fields. Thus, uncertainty estimates are not provided for these sections. However, as will be described, confidence in these sections is obtained through favorable comparisons with similar average sections from the Pacific (JMF).

A compilation of tropical Atlantic satellite drifting buoy trajectories are used to provide another estimate of near surface horizontal divergence. Data are available from 1989 to the present, with the majority of the information collected after 1992.

The buoys were deployed as contributions to both WOCE and the Tropical Ocean Global Atmosphere (TOGA) programs. The standard WOCE/TOGA buoy is drogued at 15m. Drift characteristics of the buoys have been determined and under typical tropical Atlantic wind/wave conditions the drifters exhibit a slippage

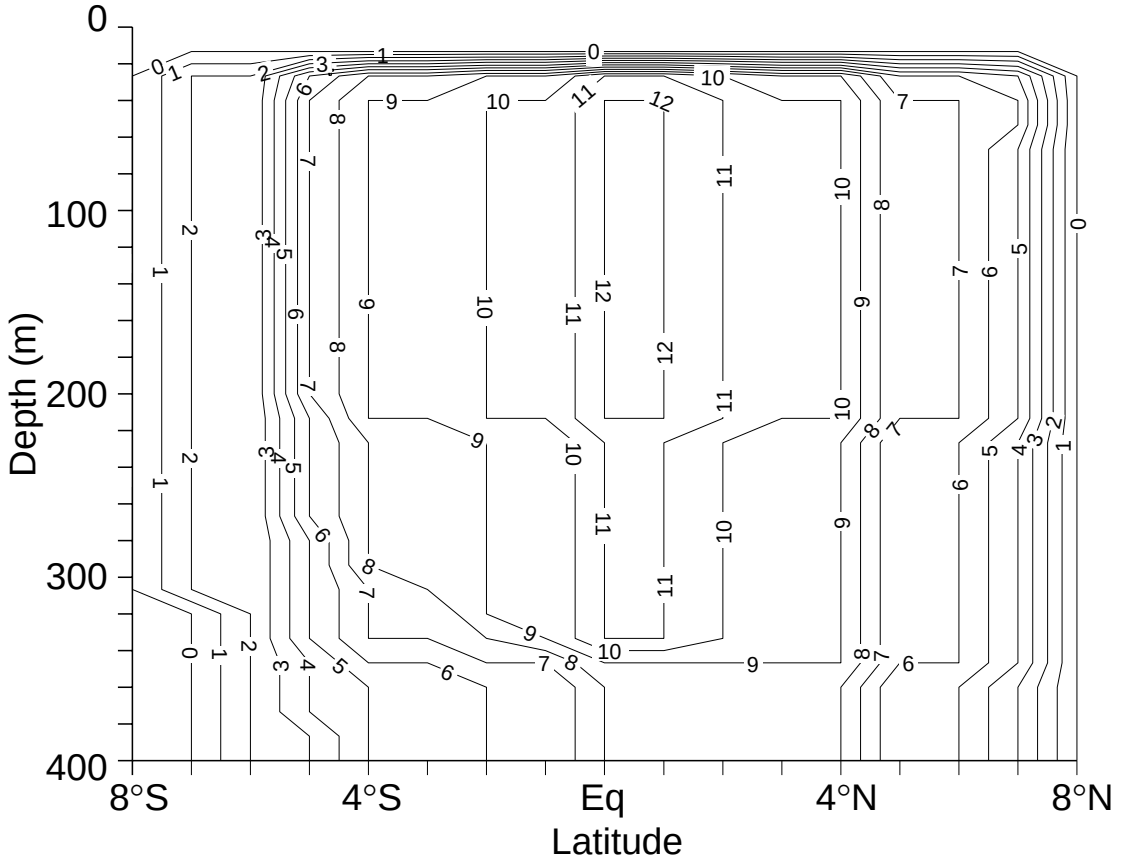

Figure 3. Data availability given as a vertical section of number of data points available on a 1.0 degree of latitude by 10m grid.

of about .01 m/s (Niller *et al*., 1995). Only buoys with drogue attached are used in the analysis. Buoy data were averaged into 1 degree of latitude by 5 degrees of longitude bins to estimate mean near-surface current structure.

The buoys were deployed as contributions to both WOCE and the Tropical Ocean Global Atmosphere (TOGA) programs. The standard WOCE/TOGA buoy is drogued at 15m. Drift characteristics of the buoys have been determined and under typical tropical Atlantic wind/wave conditions the drifters exhibit a slippage of about .01 m/s (Niller *et al*., 1995). Only buoys with drogue attached are used in the analysis. Buoy data were averaged into 1 degree of latitude by 5 degrees of longitude bins to estimate mean near-surface current structure.

3. RESULTS

Zonal velocity structure. Transports of the EUC, NEUC and SEUC can be computed directly from the average zonal current section (Figure 4). However, the individual currents experience horizontal displacements (not shown) and this

approach will underestimate the mean transport. Thus, the average transports for the three currents were obtained by averaging the individual values from the synoptic cruises. The average transports computed using this method are listed in Table 2. Zonal transports at 35ºW from Schott *et al*. (1998) and Bourles *et al*. (1999) are also given in Table 2. As some of their data were used to generate the transports in Table 2, the estimates are similar. Differences are due to slight differences in the definition of the current boundaries (e.g., Schott *et al*. (1998) and Bourles *et al*., (1999) computed transports between different sigma-theta levels). Pacific mean transports were obtained by integrating mean zonal velocities in the bottom panel of Figure 4 and also are given in Table 2. This approach may tend to underestimate transports in comparison with the method used in the Atlantic because of the smoothing required to generate the figure.

The structure (Figure 4) and transports (Table 2) of the 3 undercurrents are similar in both basins. The NEUC and SEUC are centered some 4 degrees poleward of the equator in both oceans, with much of their transport below 200m. Both EUC's are centered on the equator with maximum velocities at 100m. The Atlantic EUC extends upward to at least 30m consistent with the large number of spring cruises (i.e., spring is the typical season for eastward flow on the equator in the western Atlantic). Similarly, the absence of a strong Atlantic NECC (Figure 4) is consistent with a spring bias in the sections (Garzoli and Katz, 1983). Finally, on it's southern boundary the 35ºW section crosses the North Brazil (NBC)/North Brazil Undercurrent (NBUC) complex (Schott *et al*., 1998). The velocities in this western boundary current are higher than observed in the Pacific South Equatorial Current (SEC) at similar latitude, Figure 4. The spatial distribution of satellite tracked drifting buoy data is inhomogeneous and sparse in places (Figure 5). Average 15m currents estimated from the drifter tracks (Figure 5) include a strong NECC. Both the northern and southern branches of the SEC are evident either side of the equator. The NBC crosses the equator along the western boundary and remains intense to 5ºN.

Meridional velocity structure. Ensemble mean, meridional velocities in the surface layer and thermocline are similar in the equatorial Atlantic and Pacific (Figure 6). In the Atlantic, northward flow is observed above 50-60m, north of 1ºS and southward flow between 1ºS and 3ºS, characteristic of a near surface divergence (as described above, velocity values are extrapolated to the surface from either 30m or 40m). South of 3ºS, the intense northward flow is representative of the NBC/NBUC (not shown), which easily masks any Ekman currents that may be present.

Equatorward flow is observed in the Atlantic between about the equator and 3-4ºN and 50-60m and 200m (Figure 6). There is also equatorward flow of the same order of magnitude and in the same depth range between 0.5ºS and 2ºS. The increased northward flow south of 2ºS represents the NBC. The average meridional currents at 136ºW display a similar vertical profile (Figure 6): i.e., equatorward flow below surface poleward flow on both sides of the equator. In both basins, the maximum meridional surface currents are of the order 0.1 m/s and subsurface flows are less than 0.1 m/s.

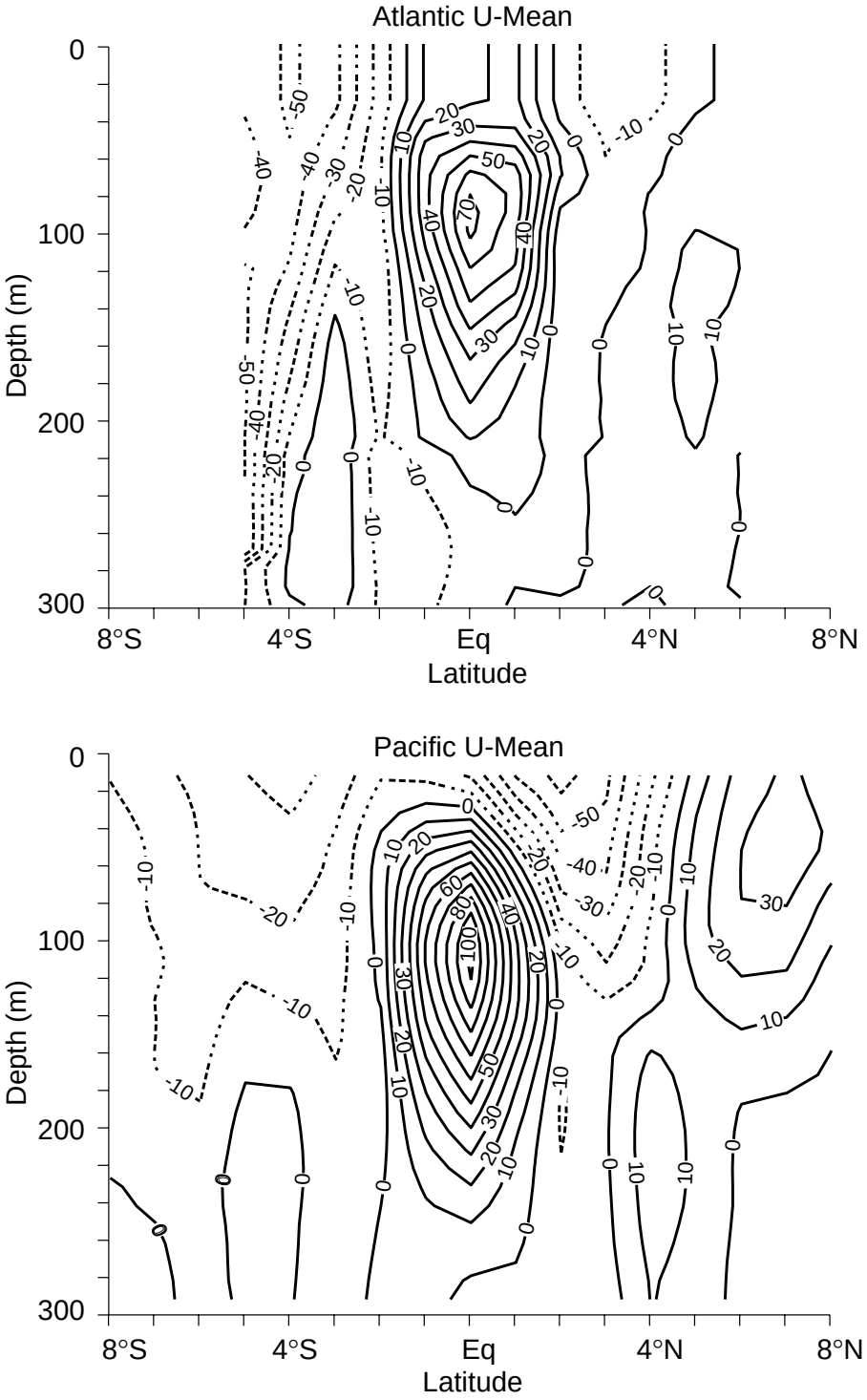

Figure 4. Mean zonal velocity (cm/s) section for the Atlantic (top panel) derived from the 12 individual sections (Figure 2) and for the Pacific (bottom panel) after JMF.

Table 2.
The South Equatorial Undercurrent (SEUC), Equatorial Undercurrent (EUC), and North Equatorial Undercurrent (NEUC) at 35°W. Average values are estimated from the individual cruises (i.e., number of values) rather than from the average section of Figure 4. Core speed is given in m/s, core depth in m, and transport in 10^6 m^3/s (=1 Sv). Transports are also given from Schott *et al.* (1998), S1998, Bourles *et al.* (1999), B1999, and Johnson *et al.* (2001), JMF-Pacific.

	Current Property	Number of Values	Average	Standard Deviation
SEUC	Core speed	8	0.21 m/s	0.09
	Core depth	8	226 m	40
	Core latitude	8	3.5 S	0.7
	Transport	8	3.8 Sv	1.0
	S 1998	4	4.6 Sv	2.1
	B 1999	3	4.1 Sv	NA
	JMF - Pacific	85	1.0 Sv	1.0
EUC	Core speed	12	0.96 m/s	0.19
	Core depth	12	84 m	27
	Core latitude	12	0.4 N	0.8
	Transport	12	23.9 Sv	5.8
	S 1998	4	22.3 Sv	3.5
	B 1999	3	16.8 Sv	NA
	JMF - Pacific	85	28.0 Sv	3
NEUC	Core speed	6	0.22 m/s	0.07
	Core depth	6	150 m	26
	Core latitude	6	4.6 N	0.8
	Transport	6	5.45 Sv	2.1
	B 1999	3	2.5 Sv	NA
	JMF - Pacific	85	4.0 Sv	1

Comparing the standard error of the mean computed from the number of observations at each grid point (Figure 3) with the mean at that point is used as a minimum measure of uncertainty (JMF). Shaded areas in Figure 6 enclose grid points where the mean is greater than the standard error. The combination of large variability and small means results in large areas where the noise is greater than the magnitude of the mean.

SADCP and drifting buoy estimates of horizontal divergence: The Atlantic and Pacific sections of mean horizontal divergence are similar (Figure 7) as to be expected from the similarities between the meridional velocity transects (Figure 6). On and close to the equator, horizontal divergences are found above 50-60m.

Nine of the ten sections that crossed the equator include this surface divergence within one degree of the equator. The mean divergences extend deeper into the water column poleward of one degree in the Atlantic and at somewhat higher latitudes in the Pacific (2ºS and 4ºN, Figure 7).

An area of subsurface equatorial convergence is observed below 50-60m in both basins (Figure 7). These convergences are caused by equatorward flows at these depths (Figure 6). There is an area of near surface convergence between 3ºN and 6ºN in the Atlantic. Of the 8 synoptic cruises that extend past 3ºN, only one does not exhibit convergence at these latitudes. In the Pacific, similar convergences exist south of 4ºS and between 6ºN and 9ºN. The large convergences south of 2ºS in the Atlantic (not shown) are related to the NBC/NBUC and would easily mask convergences caused by a southern hemisphere TC.

The effect of ignoring the $\partial u/\partial x$ component of the total divergence can be estimated using the satellite tracked drifting buoy data. Two divergence curves at 35ºW were estimated from the drifter data (Figure 5), one including the $\partial u/\partial x$ term and the other not. South of 2ºN, the two curves are quite similar in both magnitude and shape (Figure 8). Thus at least in the west-central equatorial Atlantic, the $\partial v/\partial y$ component of the total divergence is the dominant term.

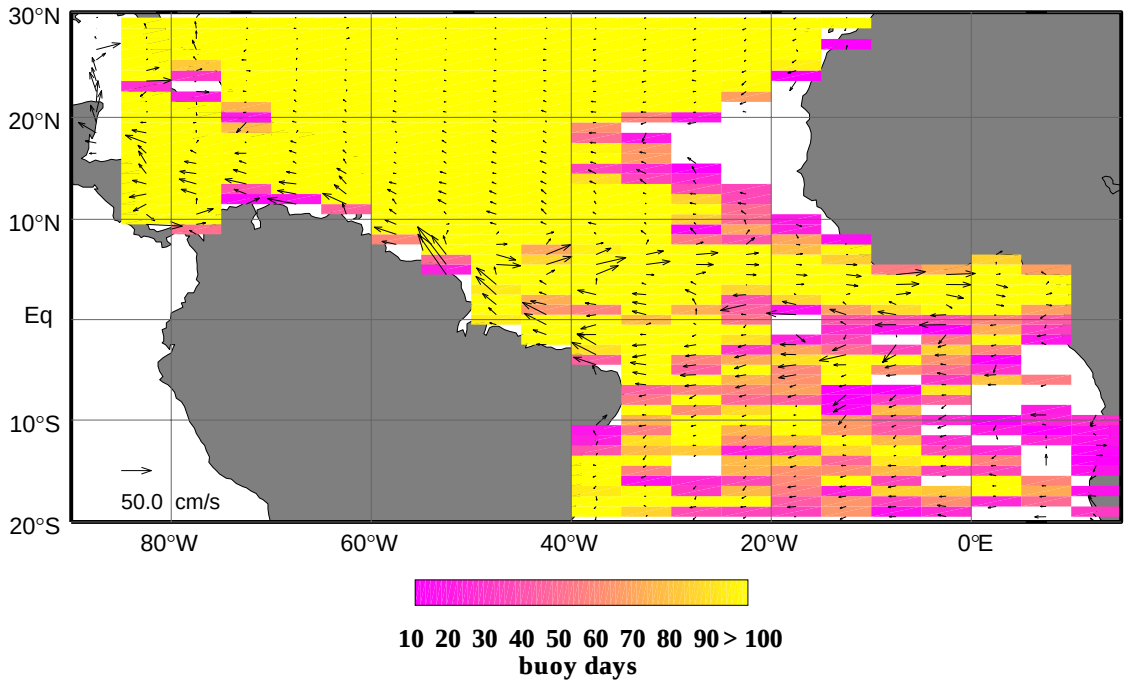

Figure 5. Mean currents at 15m computed from satellite tracked drifting buoy observations averaged onto a one degree of latitude by 5 degrees of longitude grid. Coloring indicates data availability given as number of days data are available in each quadrangle to compute velocity.

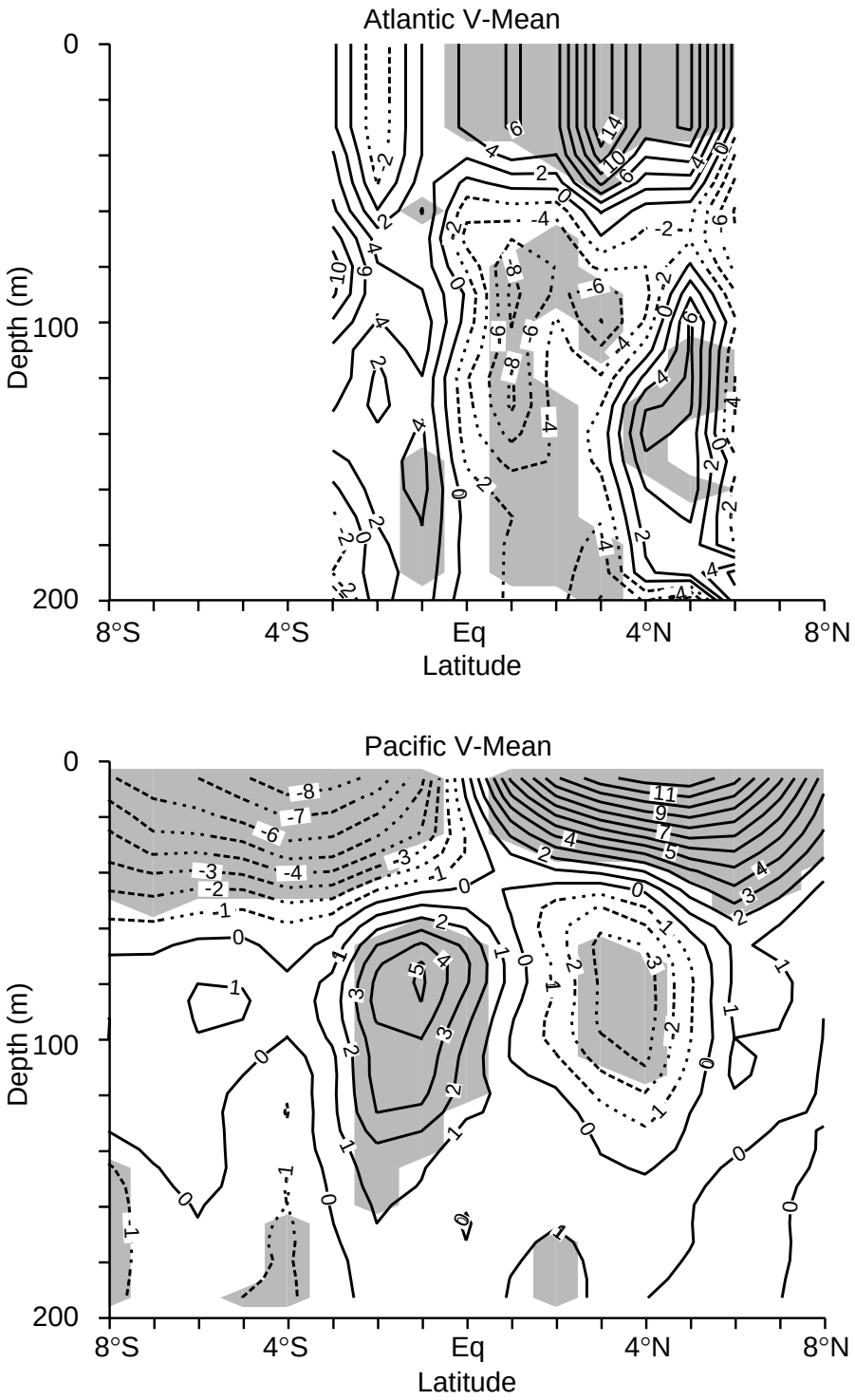

Figure 6. Mean meridional velocity (cm/s) section for the Atlantic (top panel) and for the Pacific after JMF (bottom panel). Areas where the mean meridional velocity is greater than the standard error of the mean are shaded.

Meridional velocities are extrapolated from 30m to the surface to generate the divergence distribution shown in Figure 7. Thus, SADCP divergences above 30m

(i.e., including 15m, the depth of the buoy drogues) are equivalent to divergences at this depth. The latitudinal dependence of divergence at 30m estimated from the gridded SADCP data is similar to the same curve derived from the buoy data (Figure 8). Specifically, the amplitudes of the maximum divergence are similar, and both curves have maxima at 1ºS - 0º and another at 2ºN.

Another view of the meridional structure of divergence is obtained by re-mapping the individual SADCP curves at 30m and 50 m onto a grid, which has the location of the maximum divergence rather than the equator as the zero-latitude point. The divergences from the individual cruises are then averaged with respect to this reference point and the resulting curves are shown in Figure 8.

The re-mapped divergence curves suggest minimal difference in divergence at 30 m and 50 m (not surprising because of the extrapolation of velocities from 30 m to the surface). Specifically, the curves exhibit upwelling confined to an equatorial band some 2 to 3 degrees in width bounded by bands of off-equatorial downwelling (i.e., a divergence pattern consistent with the description of TC's given in the introduction). The curve derived from the divergences of Figure 7 is different from the curve derived from the re-mapped divergences because of displacements in the latitude of maximum divergence. The latitudes of maximum divergence at 30 m range from 2ºS to 3ºN. Although the number of samples is small, 3 of the 5 maximum divergences for the March cruises are at and north of 2ºN, while 5 of the 7 divergences for the other months are between 1ºS and 1ºN.

Vertical velocity structure and estimates of equatorial upwelling: Pacific and Atlantic sections of vertical velocity are shown in Figure 9. Average equatorial upwelling occurs above 100m from 1.5ºS to 3.5ºN along 35ºW. JMF find upwelling at similar depths between 4ºS and 5ºN in the Pacific (Figure 9). Maximum upwelling velocities are about 1 to 2 $x10^{-5}$ m/s in both basins. The downwelling between 3.5º and 5ºN is taken to represent the northern boundary of the TC of the North Atlantic. As before, the location of the NBC/NBUC at 35ºW precludes the identification of a southern hemisphere TC in the Atlantic.

As with the divergences, vertical velocity was re-mapped onto a grid, which had the position of the maximum near-equatorial upwelling at 50m velocity as the zero latitude. The resulting mean properties of the equatorial upwelling and off-equatorial downwelling are given in Table 3. As expected, the maximum upwelling velocity at the equator derived from the re-mapping is larger than the maximum in Figure 9 (5.5 versus 2 $x10^{-5}$ m/s). The upwelling band is also narrower in the re-mapping (3 degrees of latitude versus 5 degrees of latitude).

4. DISCUSSION

To reiterate, because of the few sections available in this study (12 versus 85 in JMF) we chose a minimum measure of uncertainty (i.e., the magnitude of the

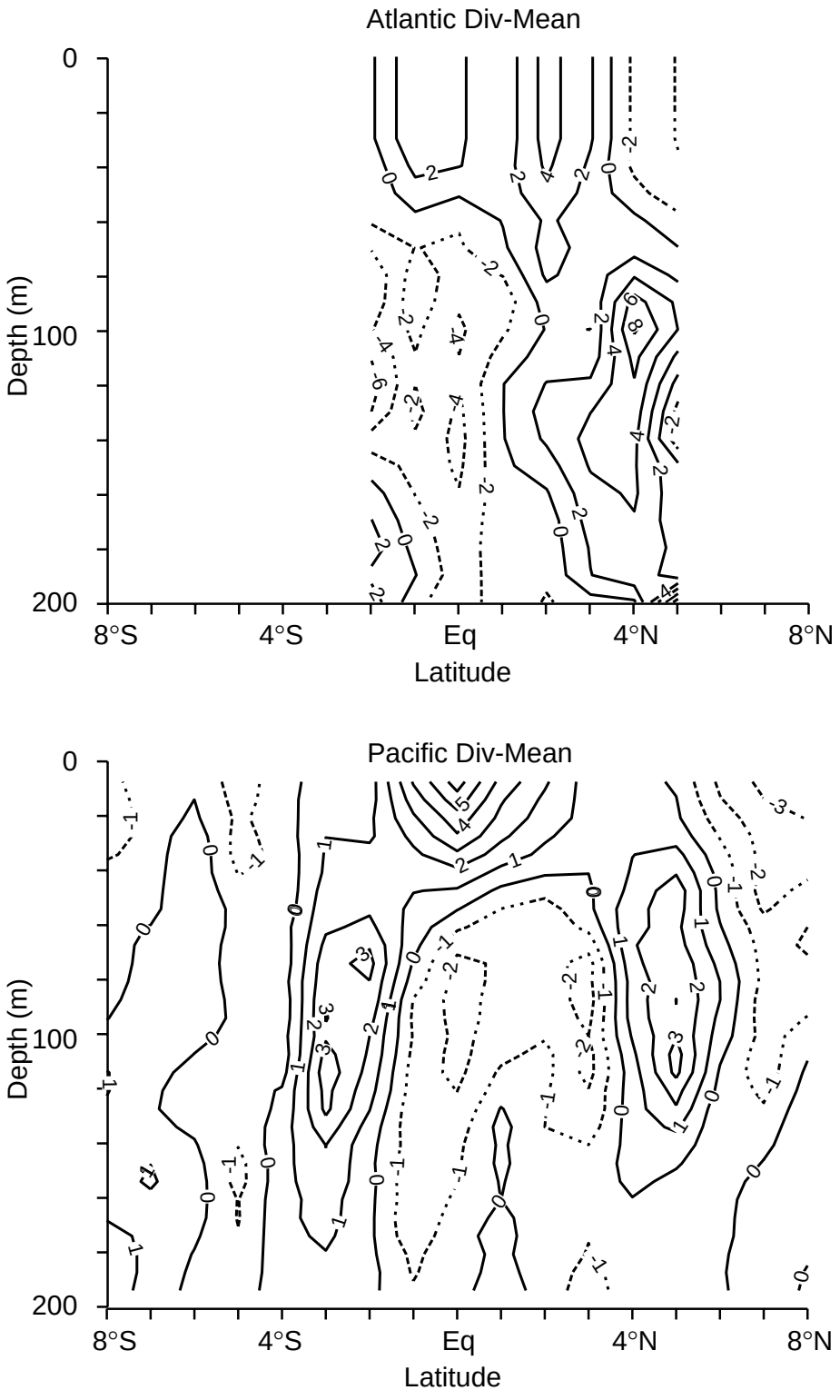

Figure 7. Mean section of horizontal divergence (10^{-7}/s) taken as $\partial v/\partial y$ in the Atlantic (top panel) and as $\partial u/\partial x + \partial v/\partial y$ for the Pacific after JMF (bottom panel).

Table 3.
Equatorial upwelling and northern hemisphere near-equatorial downwelling at 50m and 35°W. Maximum and average vertical velocities are given in 10^{-5} m/s, width of upwelling band in degrees. Transport, in 10^6 m^3/s, is computed from the width of the upwelling band and a longitudinal length of 10 degrees. There are differences in the number of values as some sections do not completely resolve the upwelling or downwelling features. Transports are not given for the off-equatorial downwelling because only one section entirely crossed this feature.

Property	**Number of Values**	**Average**	**Standard Deviation**
Equatorial Upwelling			
Maximum vertical velocity near equator	12	5.5	3.6
Latitude of maximum velocity	12	0.4°N	1.6
Width of upwelling band	8	2.8°	1.2
Average vertical velocity in upwelling band	8	3.2	1.5
Upwelling transport	8	10.8	7.5
Off-equatorial Downwelling			
Maximum vertical velocity	7	-6.5	1.5
Latitude of maximum velocity	7	3.7°N	1.3

mean is greater than the standard error of the mean) for the estimates of the mean meridional velocity shown in Figure 6. JMF assert that most of the uncertainty in their average Pacific sections is due to natural variability and not instrument noise. In the interior Atlantic, the causes of natural variability are essentially the same as in the Pacific (i.e., tropical instability waves, the seasonal cycle, planetary waves). The 12 sections available to derive the velocity property estimates are insufficient to quantify this variability and thus we (1) do not provide uncertainty measures for horizontal divergence and upwelling velocity and (2) recognize that the results presented herein are suggestive rather than conclusive.

The estimate of average equatorial upwelling velocity at 50m, 3.2×10^{-5}m/s, given in Table 3 is similar to other results. Philander and Pacanowski (1986) simulate in an ocean model a maximum equatorial vertical velocity at 30°W of 2.8×10^{-5} m/s. Weingartner and Weisberg (1991) estimated vertical velocity from a current meter array centered at 28°W. The annual average vertical velocity was a maximum at

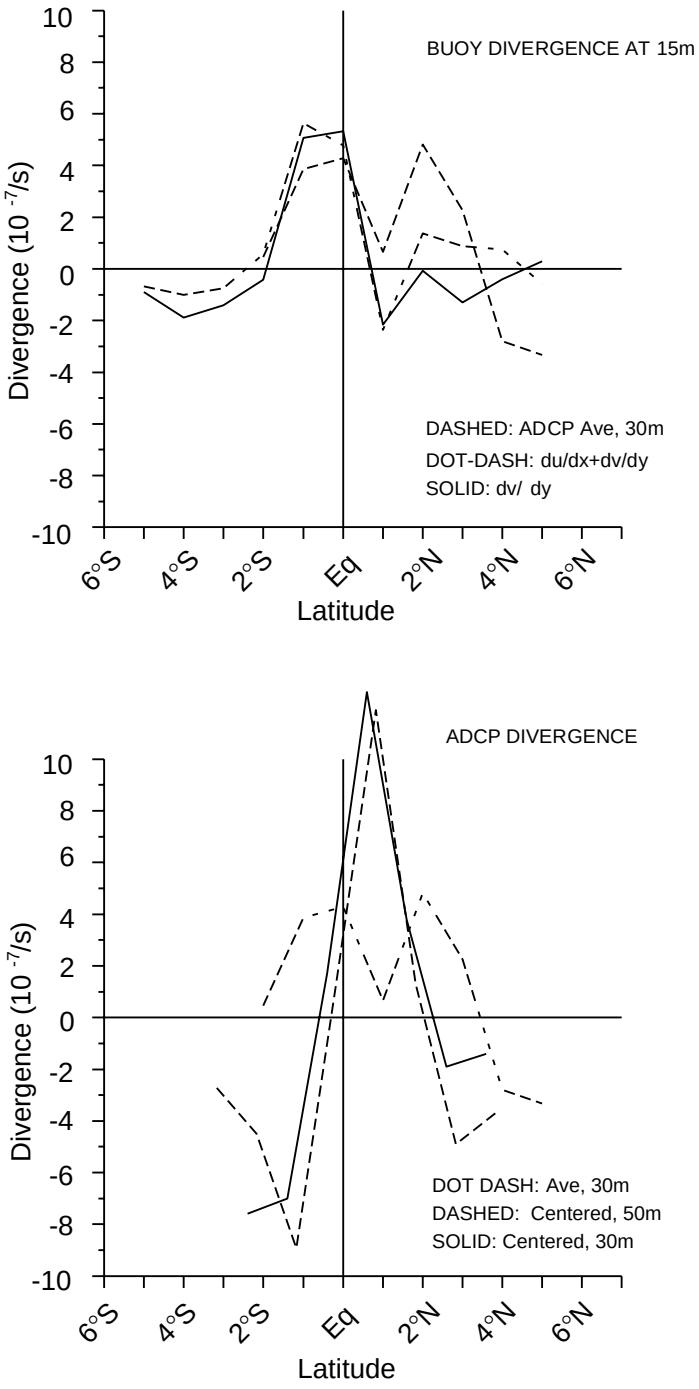

Figure 8. Comparison of horizontal divergence (10^{-7}/s) at (a) 30 m computed from the average Atlantic v-section (Figure 7), the dashed line and (b) at 15 m from drifting buoy data using only the $\partial v/\partial y$ term, solid line and both terms, dot-dash line, top panel. Comparison of horizontal divergences at 30 m from the Atlantic SADCP section (Ave. dot-dash line) of Figure 7 and 30 m (solid line) and 50 m (dashed line) computed by using the maximum equatorial upwelling position as the zero coordinate, (centered) bottom panel. The latter two curves are plotted relative to the average latitude of maximum divergence.

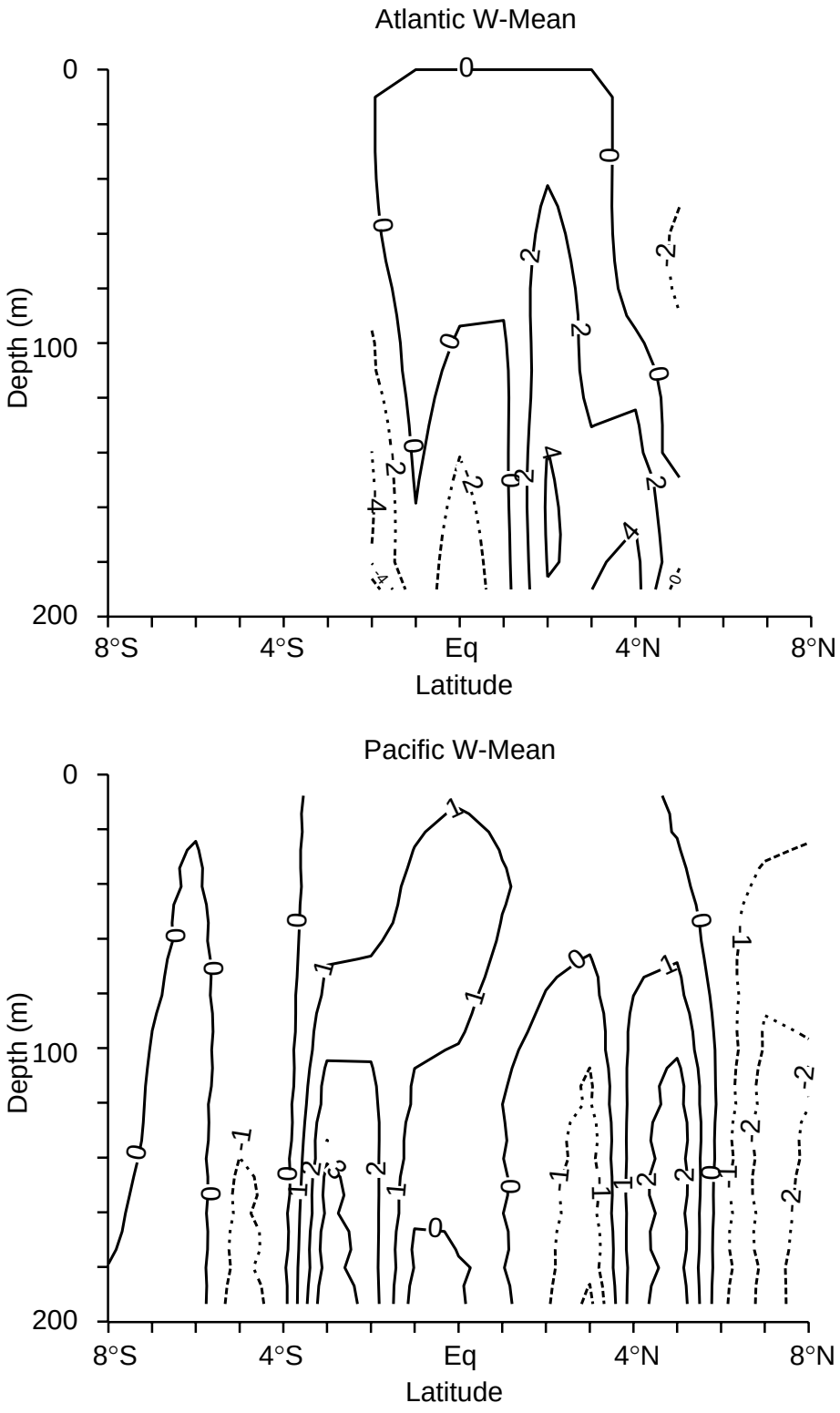

Figure 9. Mean vertical velocity (10^{-5} m/s) for the Atlantic (top panel) and Pacific after JMF (bottom panel).

about 50-60m and equal to 0.5×10^{-5} m/s. However, instantaneous maximum upwelling velocities were of the order 5×10^{-5} m/s, similar to the average maximum velocity computed from the SADCP data, Table 3. However, there are some factors and results that lend credence to the finding of a northern hemisphere TC in the Atlantic Ocean. With respect to the results presented above, the properties of horizontal velocity components (Figures 4 and 6), horizontal divergence (Figure 7) and vertical velocity (Figure 9) are very similar in both basins.

Philander and Pacanowski (1986) estimated a vertical transport through 50m in the area bounded by 2.5ºS and 2.5ºN, 30ºW and the coast of South America of 13.3 Sv. This value is similar to the 10.8 Sv we estimate from the 35ºW observations (Table 3). Gouriou and Reverdin (1992) estimated an equatorial divergence of 15 Sv between 35ºW and 4ºW.

This is a longer longitudinal band than used in the previous two estimates, but the transport is not significantly larger. However, Philander (1986) notes that during this period the equatorial Atlantic was anomalously warm, possibly coincident with anomalous upwelling.

In summary, while the evidence provided for the existence of a mean North Atlantic TC is not conclusive, we regard it as compelling and will conduct additional occupations of the 35ºW section and others farther to the east to evaluate the robustness of these results. The additional data are also needed to define the time-dependent nature of the TC. The time dependence is important as Hazeleger *et al*. find in a numerical model that high frequency variability negates of the EUC.

Acknowledgments

This work was supported by a grant to AOML from NOAA's Office of Global Programs (J. Todd, Program Manager). Comments by Dr. W. Hazeleger are greatfully appreciated. Roberta Lusic prepared the manuscript for publication.

REFERENCES

Bourles, B., Y. Gouriou, and R. Chuchla. On the circulation in the upper layer in the western equatorial Atlantic. *J. Geophys. Res*., 104, 21151-21170, 1999.

Defant, A. Die Troposphere. *Deutsche Atalantische Exed. Meteor*, 6, 289-411, 1936.

Garzoli, S. L. and E. J. Katz. The forced annual reversal of the Atlantic North Equatorial Countercurrent. *J. Phys. Ocean*.,13, 2082-2090, 1983.

Gouriou, Y. and G. Reverie. Isopycnal and diapycnal circulation of the upper Equatorial Atlantic Ocean in 1983 -1984. *J. Geophys. Res*., 97, 3543 – 3572, 1992.

Hazeleger, W., P. de Vries and Y. Friocourt. Sources of the Equatorial Undercurrent in the Atlantic in a high-resolution ocean model. To appear in: *J. Phys. Ocean.,* 2003.

Johnson, G. C. The Pacific Ocean subtropical cell surface limb. *Geophys. Res.*

Lett., 2003.

Johnson, G. C., M. .J. McPhaden and E. Firing. Equatorial Pacific Ocean horizontal velocity, divergence and upwelling. *J. Phys. Ocean.*, 31, 839-849, 2001.

Johnson E. S. and M. Luther. Mean zonal momentum balance in the upper and central equatorial Pacific Ocean. *J. Geophys. Res.*, 99, 7689-7705, 1994.

Lu, P., J. P. McCreary, Jr. and B. A. Klinger. Meridiional circulation cells and the source waters of the Pacific Equatorial Undercurrent. *J. Phys. Ocean.*, 28, 62-84, 1998.

Marin, F. and Y. Gouriou. Heat flux across 7.5N and 4.5S in the Atlantic Ocean. *Deep-Sea Res*., 47, 2111-2139, 2000.

Niller, P. P., A. Sybrandy, K. Bi, P. Poulain and D. Bitterman. Measurements of the water-following capability of Holey-sock and TRISTAR drifters. *Deep-Sea Res*. I, 42, 1591-1964, 1995.

Philander, S. G. H. Unusual conditions in the tropical Atlantic in 1984. *Nature*, 322, 236 – 238, 1986.

Philander, S. G. H. and R. C. Pacanowski. The mass and heat budget in a model of the tropical Atlantic Ocean. *J. Geophys. Res.*, 91, 14212-14220, 1986.

Schott, F. A., J. Fischer and L. Stramma. Transports and pathways of the upper-layer circulation in the western tropical Atlantic. *J. Phys. Ocean.*, 28, 1904-1928, 1998.

Sverdrup, H. U., M. W. Johnson and R. H. Fleming. The Oceans, Physics, Chemistry and General Biology, Prenitce-Hall, 1087 pp., 1942.

Weingartner, T. J. and R. H. Weisberg. A description of the annual cycle in sea surface temperature and upper ocean heat in the Equatorial Atlantic. *J. Phys. Ocean.*, 21, 83-96, 1991.

Wyrtki, K. and B. Kilonsky. Mean water and current structure during the Hawaii-to-Tahiti Shuttle Experiment. *J. Phys. Ocean.*, 14, 242-253, 1984.